

STARSPOTS - TRANSIT DEPTH RELATION OF THE EVAPORATING PLANET CANDIDATE KIC 12557548B

HAJIME KAWAHARA¹, TERUYUKI HIRANO², KENJI KUROSAKI¹, YUICHI ITO^{1,2}, AND MASAHIRO IKOMA¹

Published in ApJ Letters, 776:L6 (2013)

ABSTRACT

Violent variation of transit depths and an ingress-egress asymmetry of the transit light curve discovered in KIC 12557548 have been interpreted as evidences of a catastrophic evaporation of atmosphere with dust ($M_p \gtrsim 1M_{\oplus}\text{Gyr}^{-1}$) from a close-in small planet. To explore what drives the anomalous atmospheric escape, we perform time-series analysis of the transit depth variation of *Kepler* archival data for ~ 3.5 yr. We find a $\sim 30\%$ periodic variation of the transit depth with $P_1 = 22.83 \pm 0.21$ days, which is within the error of the rotation period of the host star estimated using the light curve modulation, $P_{\text{rot}} = 22.91 \pm 0.24$ days. We interpret the results as evidence that the atmospheric escape of KIC 12557548b correlates with stellar activity. We consider possible scenarios that account for both the mass loss rate and the correlation with stellar activity. X-ray and ultraviolet (XUV)-driven evaporation is possible if one accepts a relatively high XUV flux and a high efficiency for converting the input energy to the kinetic energy of the atmosphere. Star-planet magnetic interaction is another possible scenario though huge uncertainty remains for the mass loss rate.

Subject headings: planet-star interactions – planets and satellites: atmospheres – methods: observational

1. INTRODUCTION

Planetary evaporation is one of the most crucial factors that determines the evolution and fate of close-in planets. The atmospheric escapes of hot Jupiters have been extensively investigated from both the extreme ultraviolet observations (e.g., Vidal-Madjar et al. 2003, 2004; Lecavelier Des Etangs et al. 2010; Ehrenreich et al. 2012) and theory (e.g., Lammer et al. 2003; Baraffe et al. 2004; Yelle 2004; Lecavelier des Etangs et al. 2004; Erkaev et al. 2007; García Muñoz 2007; Murray-Clay et al. 2009). The impacts of evaporation on the evolution of even smaller planets, including super-Earths and super-Neptunes, has been also recognized (e.g. Valencia et al. 2010; Owen & Jackson 2012; Lopez et al. 2012; Owen & Wu 2013; Kurosaki et al. 2013). Recently Rappaport et al. (2012) (hereafter R12) found violent variation of transit depths and an ingress-egress asymmetry of KIC 12557548, which have been interpreted as evidences of a catastrophic evaporation of a small planet (R12, Perez-Becker & Chiang 2013, hereafter PC13). Analyzing the intensity of forward scattering, Brogi et al. (2012) and Budaj (2012) found that the dust expected as an occulter of KIC 12557548 is consistent with sub-micron grains. R12 and PC13 estimated the mass loss rate of KIC 12557548b, as $M_p \gtrsim 1M_{\oplus}\text{Gyr}^{-1}$.

However, the dominant energy source of the enormous evaporation remains unknown. One proposed possible scenario is that high bolometric energy input at the semi-major axis $a = 0.013$ AU itself produces the hydrodynamic escape. PC13 have constructed a radiative-hydrodynamic model of KIC 12557548b assuming a Parker-type wind driven by hot planetary surface with

the equilibrium temperature ~ 2000 K. They concluded that a planet with mass $M_p \lesssim 0.02M_{\oplus}$ can account for the mass loss rate of KIC 12557548b. The hydrodynamic escape driven by X-ray and ultraviolet (XUV) radiations as has been discussed for hot Jupiters is another candidate for the energy source. However, an XUV observation of the transit is impossible for KIC 12557548 with current satellites due to its distance.

Instead, we focus on the time-series of the transit depth. In this Letter, we reanalyze the *Kepler* data of KIC 12557548, but for longer period ~ 3.5 yr, than that analyzed by R12. We find the correlation between the transit depth and the modulation of the light curve using starspots. These results indicate that the evaporation of KIC 12557548b results from some energy related to the stellar activity, rather than the bolometric one.

2. ANALYSIS OF DEPTH VARIATION

We analyze archived long cadence data of KIC 12557548 between quarter 1 and 15 (Q1-Q15; ~ 3.5 yr) using the *PyKE* package to process the data (Still & Barclay 2012). Figure 1 shows the cotrended long time cadence data of KIC 12557548 (Panel A) and the flattened light curve (Panel B), extracted by *kepcotrend* and *kepflatten*. The time series of the transit depth is obtained by averaging three bins ($=1.47$ hr) around the central time of transit. We adopt the central time as $t_n = nP_{\text{orb}} + \text{offset}$, where $P_{\text{orb}} = 0.653558$ days (R12) and the offset = 2454900.352921 days. Our definition of the transit depth is the average of the 3 bins of the flatten light curve, as shown by red points in Figure 1(B). As shown in Figure 1(C), the distribution of the flatten light curve after removal of the transit periods is well fitted by a normal distribution, at least for the lower side, which verifies that our extraction method could extract almost all of the transit periods. Figure 2 shows the time series of the extracted transit depth (top) with the cotrended light curve of the star (bottom).

kawahara@eps.s.u-tokyo.ac.jp

¹ Department of Earth and Planetary Science, The University of Tokyo, Tokyo 113-0033, Japan

² Department of Earth and Planetary Sciences, Tokyo Institute of Technology, Tokyo 152-8550, Japan

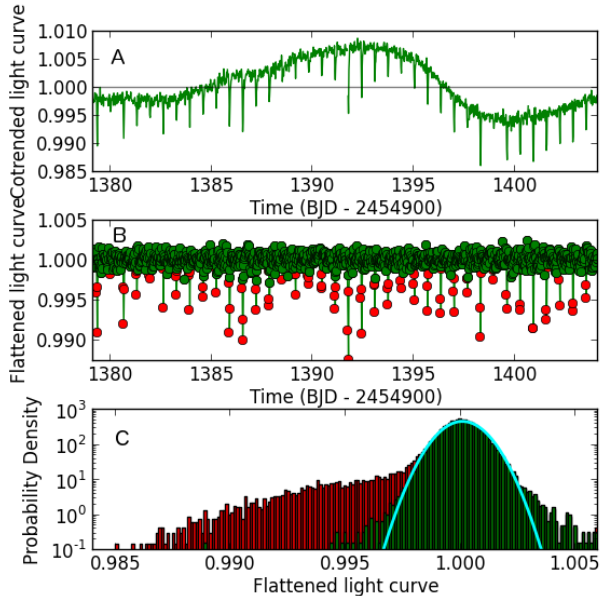


Figure 1. Panel A: part of the cotrended light curve of long time cadence of KIC 12557548. Panel B: flattened light curve and identified periods (red points) of the transits. Panel C: frequency distribution of the flattened light curve. The red tail corresponds to the transits detected by our method. The rest (green) is well fitted by a normal distribution (cyan).

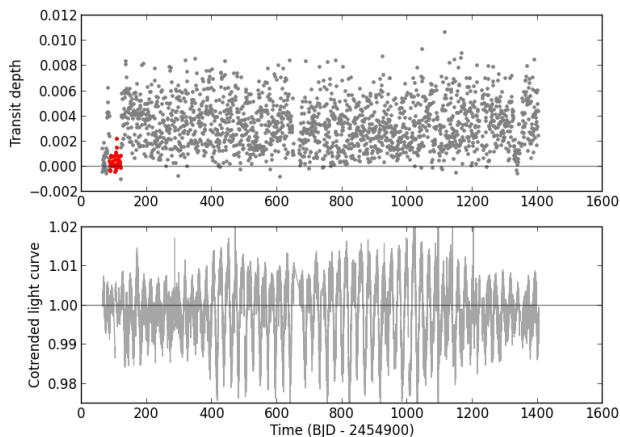


Figure 2. Transit depth variation (top) with cotrended light curve (bottom). One can see the period marked by red points in which transits are mostly undetected (see Section 3).

2.1. Periodicity of Transit Depth

Figure 3 shows Lomb-Scargle periodograms of the time series of the transit depth. We find three peaks above false alarm probability (FAP) = 0.1 %, $P_1 = 22.83 \pm 0.21$ days, $P_2 = 112.1 \pm 3.0$ days, and $P_3 = 152 \pm 7$ days, corresponding to FAP = 0.04 %, 10^{-5} %, and 6×10^{-4} %. We also compute periodogram of the cotrended light curve excluding the detected transit duration (bottom panel in Figure 3). We find the most prominent peak at $P_{\text{rot}} = 22.91 \pm 0.24$ days and its harmonic peaks.

We also performed high resolution spectroscopy for KIC 12557548 with the High Dispersion Spectrograph on the Subaru telescope. We adopted the standard

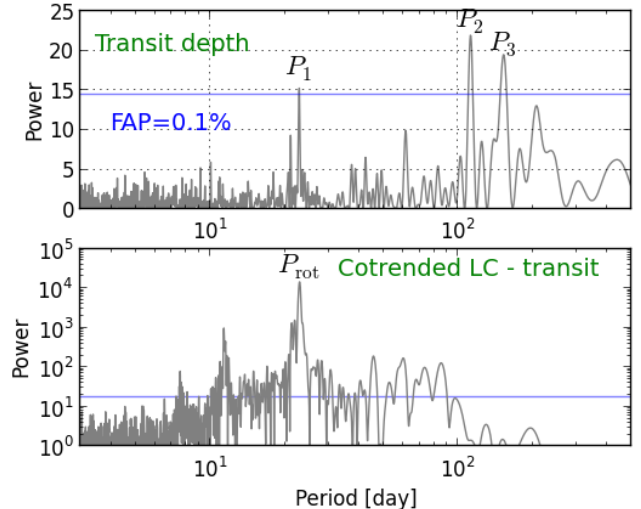


Figure 3. Lomb-Scargle periodograms of the depth variation (top) and cotrended light curve without transit duration (bottom). The vertical lines indicate the 0.1 % level of the FAP.

“Ra” setup with the image slicer No.2 ($R \sim 80,000$ and 510 – 780 nm). The basic spectroscopic parameters were extracted based on Takeda et al. (2002) and Hirano et al. (2012): $T_{\text{eff}} = 4950 \pm 70$ K, $\log g = 3.9 \pm 0.2$, $[\text{Fe}/\text{H}] = 0.09 \pm 0.09$, and $v \sin i = 1 \pm 1$ km s $^{-1}$. The resultant systematic error in $v \sin i$ is quite uncertain because of the faintness of the target star ($V \sim 16$), but we can safely rule out a large rotational velocity, $v \sin i \gtrsim 4$ km s $^{-1}$, corresponding to a rapid rotation $P_{\text{rot}} \lesssim 8$ days (we assume $R_{\star} = 0.65 R_{\odot}$; R12).

On the assumption that this value is the stellar rotation period, the shortest periodicity found in the transit depth variation $P_1 = 22.83 \pm 0.21$ days is consistent with the stellar rotation period. We concentrate on the periodicity of P_1 through the rest of the paper.

We fold the transit depth variation with P_1 (the top and middle panels in Figure 4). The mean value of binned data has ~ 30 % variation. We also fold the cotrended light curve with P_1 (the bottom panel) and find that the folded cotrended light curve is negatively correlated with the folded depth variation. A large starspot can survive for many years (Berdyugina 2005). The 2 % variation of the folded light curve can be interpreted as long term variation due to a large starspot associated with a local active area. Hence our interpretation of the anti-correlation is that the planet tends to make deeper occultation when facing the large starspot.

In general, stellar visibility depends on competition among starspots and faculae. In the case of the Sun, spot modeling (Lanza et al. 2007) predicts that a single active area decreases the visibility only for the angle between the line-of-sight and the local active area on the stellar surface $\phi \lesssim 45^\circ$ due to the large faculae-to-spots ratio $Q = 9$. However, for several stars with large flux modulation, smaller values of $Q = 1 - 4.5$ were estimated from the spot modeling and faculae for these stars do not contribute significantly to the visibility (Lanza et al. 2009b,a, 2010). Throughout the rest of the paper, we assume that the local active area decreases stellar visibility.

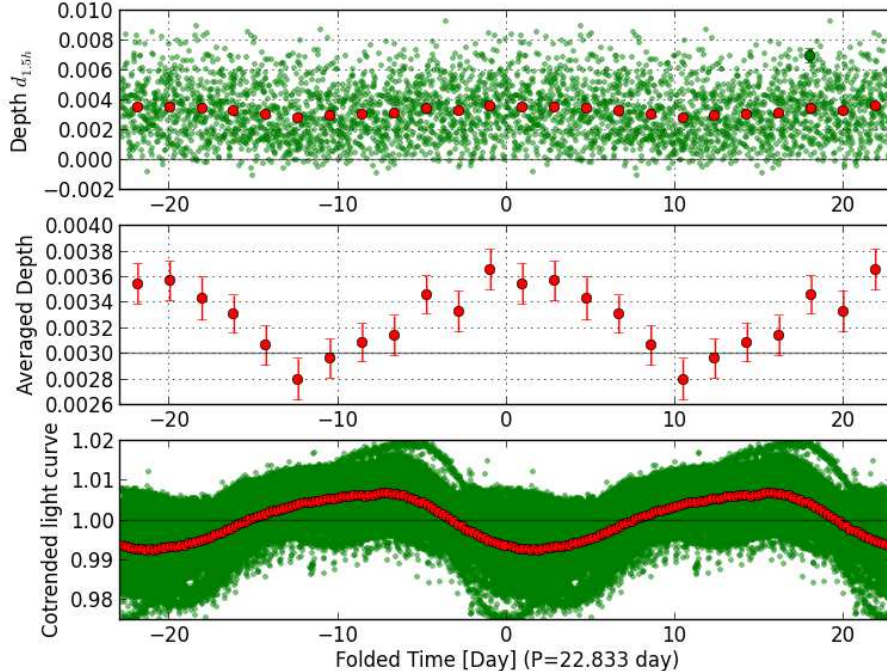


Figure 4. Top panel: the transit depth variation folded by $P_1 = 22.83 \pm 0.21$ days. A typical statistical error of the depth is shown by a green bar. Red bars are the transit depth averaged over bins. Middle panel: the mean value of the binned data of the top panel (an expanded version of the top panel around the red error bars). Bottom panel: the folded cotrended light curve of KIC 12557548.

The stellar visibility variation results in the apparent variation of the measured depth via normalization. Désert et al. (2011) considered this effect for different epochs of stellar activity (a ~ 1 year interval). We use a similar formalism although we consider this effect during one stellar rotation. The apparent variation of the depth $\delta_d \equiv (d_v - d_o)/d_o$ is related to that of the visibility during one revolution, $\delta_F \equiv (F_v - F_o)/F_o$ as

$$\delta_d = \alpha \delta_F, \quad (1)$$

where d_v and d_o are the measured depths when the active area is located on the side visible to us and the opposite side, F_v and F_o are the visibilities for the two side. Denoting the average surface brightness of photosphere by f_v and f_o for the two sides and that along the trajectory of transit by \tilde{f}_v , \tilde{f}_o , we can express

$$\delta_d = \frac{(\tilde{f}_v/f_v)}{(\tilde{f}_o/f_o)} - 1 = \frac{\delta_{\tilde{f}}/\delta_f - 1}{1 + \delta_F} \delta_F, \quad (2)$$

where $\delta_f \equiv (f_v - f_o)/f_o = \delta_F$ and $\delta_{\tilde{f}} \equiv (\tilde{f}_v - \tilde{f}_o)/\tilde{f}_o$. Assuming that the spot crossing is negligible ($|\delta_{\tilde{f}}/\delta_f| < 1$) and $1 + \delta_F \sim 1$, we obtain $-2 \lesssim \alpha \lesssim 0$. If the surface brightness outside the spot areas is homogeneous, we obtain $\alpha = -1$. In our case, we expect the 0-4 % variation of δ_d to be anti-correlated to the stellar visibility. Since the observed variation is $\delta_d \sim 30$ %, we conclude that the periodicity of the depth variation synchronized with the stellar rotation is not a false positive.

Van Eylen et al. (2013) found seasonal variation of transit depth for HAT-P-7 b due to instrumental systematics. They did not report any other periodicity < 1 yr. Since the periodicities P_2 and P_3 are larger than period of a quarter, instrumental systematics should be

considered in further studies.

3. INTERPRETATION

To consider possible scenarios of evaporation, two important constraints from observation, the mass-loss rate \dot{M}_p and the planet radius R_p , should be taken into account. The mass-loss rate was constrained by both R12 and PC13 in similar but slightly different ways, $\dot{M}_p \sim 1M_\oplus \text{Gyr}^{-1}$ and $\dot{M}_p > 0.1 - 1M_\oplus \text{Gyr}^{-1}$. Here we summarize the essential part of their derivation. The \dot{M}_p can be estimated using the total cross section of transit $S = \pi R_*^2 d = 7 \times 10^{19} \text{cm}^2$ (we adopt $d = 0.01$), dust density ρ_{dust} , typical length of optical path ΔL and typical time scale Δt ,

$$\begin{aligned} \dot{M}_p &\gtrsim (1 + \eta) \rho_{\text{dust}} S \Delta L / \Delta t \\ &= 1 \times (1 + \eta) \left(\frac{\rho_{\text{dust}}}{1 \text{g/cm}^3} \right) \left(\frac{\Delta L}{0.1 \mu\text{m}} \right) \left(\frac{\Delta t}{1 \text{hr}} \right)^{-1} M_\oplus / \text{Gyr} \end{aligned} \quad (3)$$

where η is the gas-dust ratio. R12 adopted $\Delta t = R_* v = 1.3$ hr, assuming the typical velocity of outflow $v = 10$ km/s, $\rho_{\text{dust}} = 3 \text{g/cm}^2$, and $\Delta L = 0.2 \mu\text{m}$ as a typical grain size, which yields $\dot{M}_p \sim 1(1 + \eta)M_\oplus / \text{Gyr}$. PC13 uses an orbital period of $\Delta t = P_{\text{orb}} = 15.7$ hr, $\rho_{\text{dust}} = 1 \text{g/cm}^2$, $\Delta L = 0.5 \mu\text{m}$, which results in $\dot{M}_p \sim 0.4(1 + \eta)M_\oplus / \text{Gyr}$.

The grain size estimated from the forward scattering supported $s \sim 0.1 \mu\text{m}$ (Brogi et al. 2012; Budaj 2012). We computed the auto correlation of the $d_{1,5h}$ and found a flat correlation for a time interval, $\tau < 10$ days. It supports $\Delta t < P_{\text{orb}}$. Assuming that the dust density is an order of g/cm^2 , we use $\dot{M}_p > 1M_\oplus / \text{Gyr}$ as a fiducial constraint of the mass loss rate.

Another constraint is the upper limit of R_p . Brogi et al. (2012) estimated the 1σ upper limit of the maximum planetary radius as $R_p < 1.2R_\oplus$ translating photometric accuracy of the phase folded light curve of no-transit-like feature (around the period in red in Figure 2) into the radius.

Interpreting the starspots-depth relation in a straight forward fashion, the atmospheric escape rate should correlate with the area of the active area on the stellar surface. Because the optical flux does not change much ($\sim 2\%$) and is negatively correlated with the transit depth, the bolometric radiation is unlikely to be a source of the relation.

3.1. XUV evaporation

Strong XUV radiation is often related to stellar spots since the XUV flares originate from magnetic loops. The X and/or UV periodicity with rotation were found in several stars (e.g. DeWarf et al. 2010; Scandariato et al. 2013). While the sunspots exhibit much smaller variation than KIC 12557548, an order-of-magnitude of variability in solar X-ray has been observed over a month (e.g. Stern 1998; Güdel 2004). We found a sudden 6% increase in the flux during 30 minutes similar to the flare in the short cadence data. Such a strong flare will create strong XUV variation in a timescale of hours, which might account for the transit depth variation in every transit.

However, R12 questioned whether the input energy is sufficient to account for the mass loss rate. We revisit this problem using the theoretical mass-radius relation of sub/super-Earths with several different compositions. Because of the lack of XUV observation, we manage to estimate the XUV flux of KIC 12557548 from the X-ray flux - rotation relation, which provides $L_X = 10^{27-28.5}$ erg/s for $P_{\text{rot}} = 23$ days (Pizzolato et al. 2003). Considering the fact that KIC 12557548 has a very large active area that creates 2% continuous flux variation over 3.5 yr, we adopt $L_{\text{XUV}}/L_{\text{solar}} = 10^{-5}$, corresponding to $L_{\text{XUV}} \sim 10^{28.5}$ erg/s.

In the energy-limit regime (Watson et al. 1981; Lammer et al. 2003; García Muñoz 2007; Lecavelier Des Etangs 2007), the mass loss rate can be estimated as

$$\dot{M}_p(R_p) = \epsilon \frac{\pi r_1^2 F_{\text{XUV}}}{GM_p/r_0} \frac{1}{K_{\text{tide}}}, \quad (4)$$

where r_0 is the radius where gas is bound to the planet, r_1 is the radius where the bulk of incoming XUV flux is absorbed, ϵ is the efficiency for converting the input energy to the kinetic energy of the atmosphere. Because the base level of the XUV deposition r_1 is under discussion (e.g. Baraffe et al. 2004; García Muñoz 2007; Murray-Clay et al. 2009), we adopt the radius where optical depth ~ 1 conservatively, i.e. $r_0 = r_1 = R_p$.

A correction factor for the Roche lobe effect, K_{tide} , (Erkaev et al. 2007) is given by,

$$K_{\text{tide}} = 1 - \frac{3}{2} \left(\frac{R_p}{R_H} \right) + \frac{1}{2} \left(\frac{R_p}{R_H} \right)^3, \quad (5)$$

where R_H is the Hill radius,

$$R_H \sim 3.4 \left(\frac{M_p}{M_\oplus} \right)^{1/3} \left(\frac{M_\star}{0.7M_\odot} \right)^{-1/3} R_\oplus. \quad (6)$$

On the basis of Kurosaki et al. (2013), we compute the mass-radius relation of planets composed of 100% water, 50% water+50% rocky core, 10% water+90% rocky core (volatile-rich planets), 100% rock, and 100% iron assuming the equilibrium temperature of KIC 12557548b (~ 1800 K). We neglect the contribution of a thin atmosphere, which should be evaporating, for the 100% rock and iron planets to compute the relation. The interior structure of the planet is computed with equations of hydrostatic equilibrium, mass conservation, and energy conservation (e.g. Kippenhahn & Weigert 1990) and the equation of state. A detailed description is found in Kurosaki et al. (2013).

Figure 5 (left) shows the mass-radius relation of these planets. We find that the radius of volatile-rich (the water fraction being $\gtrsim 10\%$) planets cannot be smaller than the upper limit of planetary radius $\sim 1.2R_\oplus$ because the gravity cannot bind the atmosphere. Therefore KIC 12557548b is unlikely to be a volatile-rich planet. Figure 5 (right) shows the \dot{M}_p expected in the energy-limit case, assuming the relatively high flux $L_{\text{XUV}} = 10^{-5}L_\odot$ and an assumption for the efficiency of $\epsilon = 0.5$. The density of the planet composed of iron is too dense to obtain the mass loss rate needed. The \dot{M}_p of the rocky planet is $\sim 1M_\oplus/\text{Gyr}$. The Roche lobe effect increases \dot{M}_p to two times larger than that without the tide. R12 discussed that the XUV luminosity is at least a factor of 10 too low compared to the luminosity needed assuming $\epsilon = 0.1$. The Roche lobe effect and the assumption of ϵ are likely to cause the difference by one order-of-magnitude in \dot{M}_p between R12 and us. Hence, a rocky planet is possible as a candidate for KIC 12557548b.

One might consider that volatile components on the rocky planet increase the planetary effective radius and \dot{M}_p . We derive the surface pressure needed to increase the transit radius R_t to χ times of the radius of the silicate core R_b ($R_t = R_b + h = (1 + \chi)R_b$) though the observed transit radius is not identical to the effective radius for equation (4). We adopt $\chi = 0.5$, i.e. ~ 2 times larger cross section. The atmospheric height from the ground to the point where the optical depth through the planetary limb is unity is estimated by assuming an isothermal atmosphere with temperature T and a power-law dependence of the opacity on pressure ($\kappa \propto P^\gamma$; Rogers & Seager 2010),

$$h = \frac{H}{\gamma + 1} \log \left(\frac{\tau_b}{\tau(r)} \right) \quad (7)$$

where $H = kT/\mu m_H g$ is the pressure scale height, P_b , μ and m_H are the surface pressure at the lower boundary, mean-molecular weight and proton mass. The vertical optical depth $\tau(r)$ is linked to the optical depth of the chord (e.g. Burrows et al. 2007; Hansen 2008; Rogers & Seager 2010) as

$$\tau_t(r) \approx \sqrt{\frac{2\pi(\gamma + 1)r}{H}} \tau(r). \quad (8)$$

It yields

$$h = \frac{H}{\gamma + 1} \log \left(\sqrt{\frac{2\pi(h + R_b)}{H(\gamma + 1)}} \frac{\kappa_b P_b}{g} \right), \quad (9)$$

where κ_b is the visible opacity at the surface. Then we

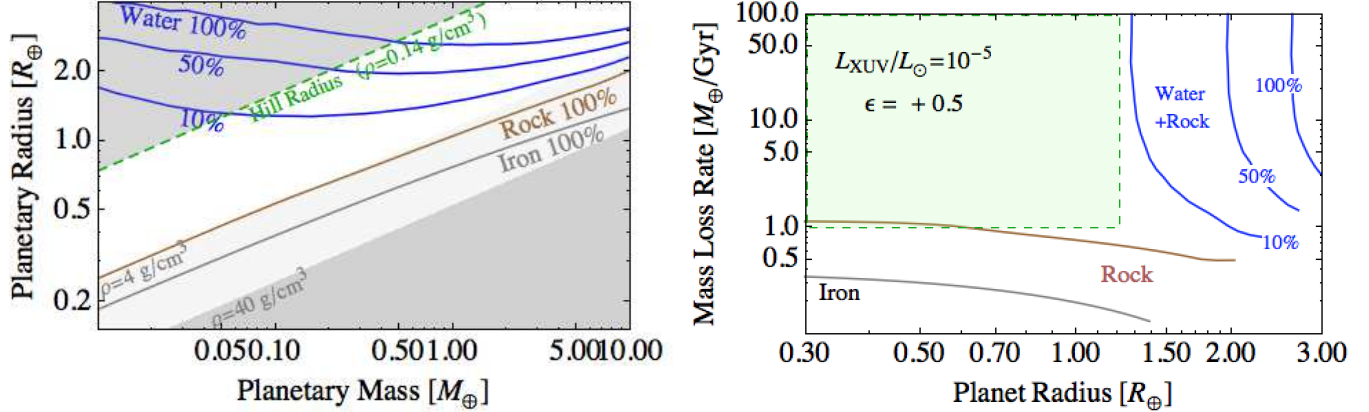


Figure 5. The mass-radius relation (left) and \dot{M}_p in the energy-limited regime assuming the XUV driven escape (right). In the left panel, a green dashed line indicates the hill radius assuming $M_* = 0.7M_\odot$ and $a = 0.013$ AU. In the right panel, fiducial constraints derived by the minimum transit depth and the mass loss estimate are shaded by green. We assume relatively high value of the XUV flux $L_{XUV} = 10^{-5} L_\odot$ and high efficiency $\epsilon = 0.5$.

obtain

$$P_b = \sqrt{\frac{\gamma+1}{\chi+1}} \frac{g}{\kappa_b} \frac{e^{\chi(\gamma+1)\lambda_b}}{\sqrt{2\pi\lambda_b}} \sim 10^{0.4\chi(\gamma+1)\lambda_b - \Delta} \left(\frac{\kappa_b}{1 \text{ cm}^2/\text{g}} \right)^{-1} [\text{bar}] \quad (10)$$

where $\lambda_b \equiv GM\mu m_H/kTR_b$ is the escape parameter and $\Delta \sim 4.5$ for $M = (0.01 - 1)M_\oplus$ and $\rho = 4 \text{ g/cm}^3$. For the Na atmosphere, which is a possible dominant component of the atmosphere of the rocky planets (e.g. Miguel et al. 2011), $\bar{\kappa}_b \sim 10^2(P/1\text{bar})^1$ for $10^{-2} - 10^3$ bar, where we computed $\kappa_b(\lambda)$ based on Atomic Line Data (Kurucz & Bell 1995) with the method by Piskunov & Kupka (2001) and took the logarithm average of $\kappa_b(\lambda)$ (see Eq. [9]) for the *Kepler* band. Adopting $\mu = 30$, we obtain $P_b \sim 10$ bar and 1 bar for $M = 0.1M_\oplus$ ($\lambda_b \sim 24$) and $M = 0.01M_\oplus$ ($\lambda_b \sim 5$), which are much higher than the equilibrium vapor pressure of the olivine, $10^{-5} - 10^{-2}$ bar for 2000-2500 K (Perez-Becker & Chiang 2013) (see also Miguel et al. 2011). Thus the Na atmosphere vaporized at the equilibrium temperature is unlikely to increase the cross section of XUV. Though we assumed the equilibrium temperature as the surface temperature for simplicity, further study of the atmospheric structure over magma ocean is needed to derive the realistic contribution of the volatile components.

3.2. Energetic Electron by Magnetic Reconnection

Star-planet magnetic interaction is another possible scenario for a catastrophic evaporation that correlates with stellar activity. Recently Lanza (2013) proposed a new scenario in which energetic electrons released by magnetic reconnection at the boundary of the planetary magnetosphere inject kinetic energy into the planetary atmosphere. The power released by the reconnection per area, corresponding flux, is estimated (Lanza 2012, 2013) as

$$F_{\text{mag}} \equiv \frac{P_{\text{mag}}}{\pi R_p^2} = \frac{B_0^2}{2\mu_B} \sqrt{\frac{GM_*}{a}} \left(\frac{B_p}{B_0} \right)^{2/3} \left(\frac{R_*}{a} \right)^{4s/3} \quad (11)$$

where μ_B is the magnetic permeability of the plasma, B_0 and B_p are the magnetic field at the pole of a star and a planet. If adopting $B_0 = 10$ G, $B_p = 1$ G, and $s = 2$, we obtain $4\pi a^2 F_{\text{mag}} = 5 \times 10^{-5} (\mu_B/\mu_0)^{-1} L_\odot$, (μ_0 is the vacuum permeability). Since this value is larger than our fiducial value of $L_{XUV} = 10^{-5} L_\odot$ in Section 3.1, it is possible to account for the mass loss rate.

4. SUMMARY

We performed a time-series analysis of the transit depth of KIC 12557548b. We found that the transit depth variation has three values of specific periodicity above FAP=0.1 % and that the shortest one $P_1 = 22.83 \pm 0.21$ days is consistent with the stellar rotation period estimated by visibility modulation. We interpreted these results as evidence that the evaporation is related to stellar activity.

Using the theoretical mass-radius relation with tide, we showed that the massive escape of a rocky planet driven by XUV is possible if assuming high XUV flux and high efficiency. The energetic electrons released by the magnetic reconnection is another possible scenario. Though we could not identify any plausible scenario to account for the $\sim 1M_\oplus/\text{Gyr}$ evaporation correlated with stellar activity, future XUV observations will enable us to understand what type of energy evaporates close-in small planets, if transiting planet surveys such as *Transiting Exoplanet Survey Satellite* find nearby similar systems.

We thank Yoichi Takeda for helping with the spectroscopic analysis. This work is supported by the Astrobiology Project of the CNSI, NINS (AB251009) and by Grant-in-Aid for Scientific research from JSPS and from the MEXT (Nos. 25800106, 25400224, and 25-3183).

REFERENCES

- Baraffe, I., Selsis, F., Chabrier, G., Barman, T. S., Allard, F., Hauschildt, P. H., & Lammer, H. 2004, *A&A*, 419, L13
 Berdyugina, S. V. 2005, *Living Reviews in Solar Physics*, 2, 8
 Brogi, M., Keller, C. U., de Juan Ovelar, M., Kenworthy, M. A., de Kok, R. J., Min, M., & Snellen, I. A. G. 2012, *A&A*, 545, L5
 Budaj, J. 2012, arXiv:1208.3693
 Burrows, A., Hubeny, I., Budaj, J., & Hubbard, W. B. 2007, *ApJ*, 661, 502
 Désert, J.-M., et al. 2011, *A&A*, 526, A12

- DeWarf, L. E., Datin, K. M., & Guinan, E. F. 2010, *ApJ*, 722, 343
- Ehrenreich, D., et al. 2012, *A&A*, 547, A18
- Erkaev, N. V., Kulikov, Y. N., Lammer, H., Selsis, F., Langmayr, D., Jaritz, G. F., & Biernat, H. K. 2007, *A&A*, 472, 329
- García Muñoz, A. 2007, *Planet. Space Sci.*, 55, 1426
- Güdel, M. 2004, *A&A Rev.*, 12, 71
- Hansen, B. M. S. 2008, *ApJS*, 179, 484
- Hirano, T., Sanchis-Ojeda, R., Takeda, Y., Narita, N., Winn, J. N., Taruya, A., & Suto, Y. 2012, *ApJ*, 756, 66
- Kippenhahn, R., & Weigert, A. 1990, *Stellar Structure and Evolution*
- Kurosaki, K., Ikoma, M., & Hori, Y. 2013, arXiv:1307.3034
- Kurucz, R., & Bell, B. 1995, *Atomic Line Data* (R.L. Kurucz and B. Bell) Kurucz CD-ROM No. 23. Cambridge, Mass.: Smithsonian Astrophysical Observatory, 1995., 23
- Lammer, H., Selsis, F., Ribas, I., Guinan, E. F., Bauer, S. J., & Weiss, W. W. 2003, *ApJ*, 598, L121
- Lanza, A. F. 2012, *A&A*, 544, A23
- Lanza, A. F. 2013, arXiv:1307.2341
- Lanza, A. F., et al. 2009a, *A&A*, 506, 255
- Lanza, A. F., et al. 2010, *A&A*, 520, A53
- Lanza, A. F., Bonomo, A. S., & Rodonò, M. 2007, *A&A*, 464, 741
- Lanza, A. F., et al. 2009b, *A&A*, 493, 193
- Lecavelier Des Etangs, A. 2007, *A&A*, 461, 1185
- Lecavelier Des Etangs, A., et al. 2010, *A&A*, 514, A72
- Lecavelier des Etangs, A., Vidal-Madjar, A., McConnell, J. C., & Hébrard, G. 2004, *A&A*, 418, L1
- Lopez, E. D., Fortney, J. J., & Miller, N. 2012, *ApJ*, 761, 59
- Miguel, Y., Kaltenecker, L., Fegley, B., & Schaefer, L. 2011, *ApJ*, 742, L19
- Murray-Clay, R. A., Chiang, E. I., & Murray, N. 2009, *ApJ*, 693, 23
- Owen, J. E., & Jackson, A. P. 2012, *MNRAS*, 425, 2931
- Owen, J. E., & Wu, Y. 2013, arXiv:1303.3899
- Perez-Becker, D., & Chiang, E. 2013, *MNRAS*
- Piskunov, N., & Kupka, F. 2001, *ApJ*, 547, 1040
- Pizzolato, N., Maggio, A., Micela, G., Sciortino, S., & Ventura, P. 2003, *A&A*, 397, 147
- Rappaport, S., et al. 2012, *ApJ*, 752, 1
- Rogers, L. A., & Seager, S. 2010, *ApJ*, 712, 974
- Scandariato, G., et al. 2013, *A&A*, 552, A7
- Stern, R. A. 1998, in *Astronomical Society of the Pacific Conference Series*, Vol. 154, *Cool Stars, Stellar Systems, and the Sun*, ed. R. A. Donahue & J. A. Bookbinder, 223
- Still, M., & Barclay, T. 2012, *PyKE: Reduction and analysis of Kepler Simple Aperture Photometry data*, *Astrophysics Source Code Library*
- Takeda, Y., Ohkubo, M., & Sadakane, K. 2002, *PASJ*, 54, 451
- Valencia, D., Ikoma, M., Guillot, T., & Nettelmann, N. 2010, *A&A*, 516, A20
- Van Eylen, V., Lindholm Nielsen, M., Hinrup, B., Tingley, B., & Kjeldsen, H. 2013, arXiv:1307.6959
- Vidal-Madjar, A., et al. 2004, *ApJ*, 604, L69
- Vidal-Madjar, A., Lecavelier des Etangs, A., Désert, J.-M., Ballester, G. E., Ferlet, R., Hébrard, G., & Mayor, M. 2003, *Nature*, 422, 143
- Watson, A. J., Donahue, T. M., & Walker, J. C. G. 1981, *Icarus*, 48, 150
- Yelle, R. V. 2004, *Icarus*, 170, 167